Implementation of the IEC TS 60904-1-2 Measurement Methods for Bifacial Silicon PV Devices

Juan Lopez-Garcia, Ebrar Ozkalay, Robert P. Kenny, Laura Pinero-Prieto, David Shaw, Diego Pavanello, and Tony Sample

***Abstract*—Bifacial crystalline Silicon (Si) photovoltaic (PV) devices are attracting considerable interest from manufacturers and the market since they can enhance the performance in comparison with traditional monofacial PV devices. Technical specification IEC TS 60904-1-2 was published in 2019 and proposes several characterization methods for bifacial PV device testing based on single-side, double-sided and natural sunlight illumination. This article analyses the advantages, disadvantages, the suitability and the feasibility of the different methods and compares the electrical performance obtained by the proposed approaches at the European Solar Test Installation for the testing of bifacial Si devices. Deviations in $P_{\max}$ below 0.9% for the different testing methods under test was obtained except for the double-source approach with a rear reflector (2.59%) where the measurement of the rear irradaince influence the $\underline{P}_{\max}$.**

***Index Terms*—Bifacial, photovoltaic (PV) performance, standards.**

I. Introduction

BIFACIAL crystalline silicon (Si) photovoltaic (PV) devices have emerged as a competitive and promising technology because they can produce additional output energy in comparison to conventional monofacial modules. This is due to the fact that both sides of the cell/module, can absorb solar radiation, utilizing the scattered light from the ground and surroundings. The market share of bifacial PV modules has grown significantly over the last years and is rapidly overtaking the monofacial PV modules [1]. Bifacial PV devices [in combination with horizontal single axis tracking(HSAT] leads to lowest possible levelized cost of electricity and have reached recently record electricity generation cost well below 1.5 USDct/kWh in the Middle East North African states [2]–[4]. The International Technology Roadmap for PV reported that as of 2020 bifacial modules account for about 12% of the total world PV market and anticipated that the bifacial c-Si technology in bifacial modules is expected to achieve a 40% market share in 2025 and 55% in 2031 [5].

In order to assess the PV module performance and quality, modules are characterized under standard test conditions (STCs) as defined by the International Electrotechnical Commission (IEC) [6]. To face the standardization problem on how to correctly measure and label a bifacial PV device, the IEC published in 2019 the technical specification (TS) IEC TS 60904-1-2 for the measurement of current-voltage characteristics of bifacial PV devices [7]. This TS sets limits on permissible deviations of operating conditions, provides a guideline on measurement and defines three different characterization approaches including single-side illumination with a solar simulator (measurements at equivalent irradiance levels) [8], double-sided (simultaneous illumination of both sides using double-source simulators or single-source illumination with a diffuse rear reflector or tilted mirrors) [9] and natural sunlight [10], [11]. TSs have a limited validity of three years, after which point they have to be re-assessed by the technical committee and may either be re-confirmed (for a further three years), amended or revised, converted to a full international standard or withdrawn. In this period, users of the TS are encouraged to test the appropriateness of the test methods. The European Solar Test Installation (ESTI) is an ISO/IEC 17025:2017 accredited calibration laboratory for PV and has recently extended the scope of its accreditation to encompass, for the first time worldwide, calibration of bifacial PV devices according to the IEC TS 60904-1-2 [*I–V* measurements of bifacial PV modules with single-side illumination using a pulsed solar simulator (PSS)]. This method can be used as good reference point for the evaluation of other approaches.

PV modules are typically sold in terms of their nominal peak power at STC, which is shown on the PV module nameplate and is used to estimate the power or energy delivered by installed PV systems. Due to the ever-increasing scale of PV deployment worldwide, even small improvements in performance testing can have a significant impact on system economics. Therefore, the PV sector requires accurate and reliable assessment of electrical performance adapted for both existing and innovative cell/module concepts and technologies. The rapid technical evolution needs to be matched by international standards that dictate

Manuscript received November 5, 2021; revised January 28, 2022 and March 13, 2022; accepted March 16, 2022. Date of publication April 12, 2022; date of current version April 21, 2022. This work was supported in part by the project (PV-ENERATE) which contributed to this article has received funding from the EMPIR programme co-financed by the Participating States and from the European Union's Horizon 2020 research and innovation programme. *(Corresponding author: Robert Kenny.)*

The authors are with the European Commission, Joint Research Centre, 21027 Varese, Italy (e-mail: juanlopezgarcia1981@gmail.com; ebrar.oezkalay@supsi.ch; robert.kenny@ec.europa.eu; laura.pinero@gmail.com; david.shaw@ec.europa.eu; diego.pavanello@ec.europa.eu; tony.sample@ec.europa.eu).

Color versions of one or more figures in this article are available at https://doi.org/10.1109/JPHOTOV.2022.3161186.

Digital Object Identifier 10.1109/JPHOTOV.2022.3161186

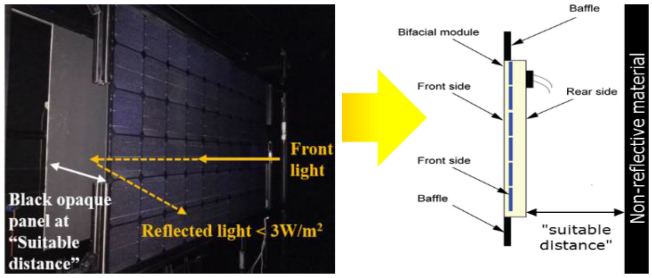

Fig. 1. Indoor setup for single-side illumination method with pulsed simulator.

the acceptable tolerances for measurements to ensure product quality, reliability and sustainability [12], as well as transparent market conditions. In this way, the entire PV community has to be involved in the testing of PV concepts such as bifacial devices that need to be in compliance with the proposed standard and need to be based on solid and reliable indoor and outdoor measurements.

This article analyses and compares the electrical performance obtained by different characterization methods used at ESTI for the testing of a bifacial Si minimodule. Such understanding will be necessary for future revision or extension of IEC TS 60904-1-2.

II. IEC TS 60904-1-2: Characterization Methods

The first approach considered in the IEC TS 60904-1-2 for measuring bifacial PV devices is based on the independent measurement of both sides at STC by means of a single source solar simulator with adjustable irradiance levels with less than 5% of nonuniformity, covering the nonilluminated side of the module by a nonreflective material(see Fig. 1). This is by far the most used method for the characterization of bifacial PV devices [13]–[15]. IEC TS 60904-1-2 states that the contribution from the light incident on the opposite side of the device under test must be eliminated during the measurement, considering a nonirradiating background when the irradiance on the surface under test does not exceed 3 W/m^2, at any point, on the nonexposed side of the device. The IEC TS 60904-1-2 defines bifaciality as the ratio between the main characteristics of the rear and front side of a bifacial device, typically at STC, quantified by specific bifaciality coefficients for short-circuit current, open-circuit voltage and output power, φ_{Isc}, φ_{Voc}, and $\varphi_{P\max}$, respectively. For example $\varphi_{P\max}$ is defined as

$$\varphi_{P\max}(\%) = \frac{P_{\max\,\mathrm{Rear}}}{P_{\max\,\mathrm{Front}}} \cdot 100 \tag{1}$$

where $P_{\max\ \mathrm{Rear}}$ (W) and $P_{\max\ \mathrm{Front}}$ (W) are the module output power measured when illuminating only the rear and the front side at STC, respectively, with a black panel covering the nonilluminated side. The minimum value between the short circuit current bifaciality φ_{Isc}, and the maximum power bifaciality coefficient $\varphi_{P\max}$ is defined as the module bifaciality. The gain in the power generation yielded by the rear irradiance on the bifacial device is calculated as a function of the rear side irradiance level. The TS states that the $P_{\max}$ of the device must be measured, at least, at two equivalent irradiance levels G_{Ei} on the front by adjusting the solar simulator intensity. This corresponds to 1000 W/m^2 on the front side plus different rear side irradiance levels G_{Ri}. The equivalent irradiance levels are determined as follows:

$$G_{Ei} = 1000 + \varphi \cdot G_{Ri}\ (\mathrm{W/m^2}) \tag{2}$$

$$\varphi = \min\left(\varphi_{Isc}, \varphi_{P\max}\right) \tag{3}$$

where φ is the minimum value between φ_{Isc} and $\varphi_{P\max}$. The rear irradiance driven power gain yield BiFi is the slope derived from the linear fit of the $P_{\max}$ versus G_R that is forced to cross the $P_{\max}$ at P_{maxSTC}. Two specific $P_{\max}$ values have to be reported, $P_{\mathrm{maxBiFi100}}$ and $P_{\mathrm{maxBiFi200}}$, for $G_{\mathrm{R1}} = 100$ W/m^2 and $G_{\mathrm{R2}} = 200$ W/m^2, respectively, obtained by linear interpolation of the data series $P_{\max}$ versus G_R according to

$$P_{\mathrm{maxBiFi10}} = P_{\mathrm{maxSTC}} + \mathrm{BiFi} \cdot 100 \tag{4}$$

$$P_{\mathrm{maxBiFi20}} = P_{\mathrm{maxSTC}} + \mathrm{BiFi} \cdot 200. \tag{5}$$

These values, bifaciality, BiFi, STC values and at least two front equivalent irradiance levels need to be reported for bifacial PV devices.

The second approach is based on the simultaneous illumination of both sides of the bifacial device with 1000 W/m^2 on the front and at least two different rear side irradiance levels G_{Ri} (i = 1, 2, 3…, for instance, $G_{R1} < 100$ W/m^2, 100 W/m^2 $< G_{R2} <$ 200 W/m^2 and $G_{R3} >$ 200 W/m^2). From these values, BiFi coefficient is calculated. Different setups have been considered: the measurement with a *double-source solar simulator* is considered in the IEC TS 60904-1-2 as a suitable method for double-sided illumination. However, this approach presents some problems at the module scale such as the logistics of timing two flashes, controlling the reflection of the environment and the added cost of using two controlled light sources instead of one [9], [16], [17]; *tilted mirrors* allow for a simultaneous measurement of both sides with a single flash from the front and two mirrors (typically aluminum or silver coated reflector) with metallic grid filters to attenuate the incident light on the backside of the module [18]–[20]*;* and by using a PSS and a *diffuse reflector* placed at a specific distance behind the module with a known reflectivity (for example, a reflective white rear sheet). This setup consisting of a reflective rear surface parallel to the module has been recently considered and studied by several groups due to its potential simulation of real outdoor direct light, albedo, and self-shading [17], [21]. However, this setup has several problems, such as rear irradiance nonuniformity, specifications of the reflector material and placement, resulting in a difficult implementation. In a recent survey performed by Newman *et al.* [16], among 13 research institutes, industry and manufacturers most of the participants scored this setup highly as a possible way to mimic real-world conditions clearly. Similarly, for indoor characterization using double-source illumination, the nonuniformity should be less than 5% of the irradiance level on both sides. The IEC TS 60904-1-2 suggests: "Reflections between the two light sources may add irradiance nonuniformity. This may generate significant offsets between single-side and double-sided measurement methods results. In this case, double-sided illumination results must be

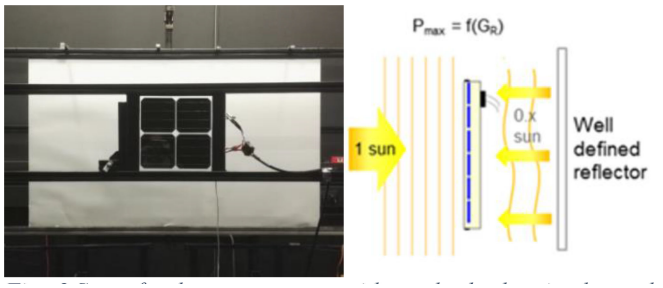

Fig. 2. Setup for the measurement with a PSS plus a white reflective rear panel.

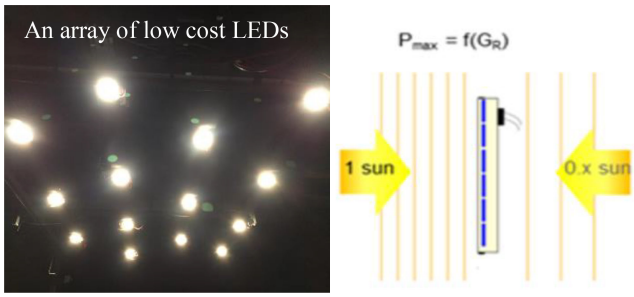

Fig. 3. Prototype of LED-based bias light with a large area pulsed simulator.

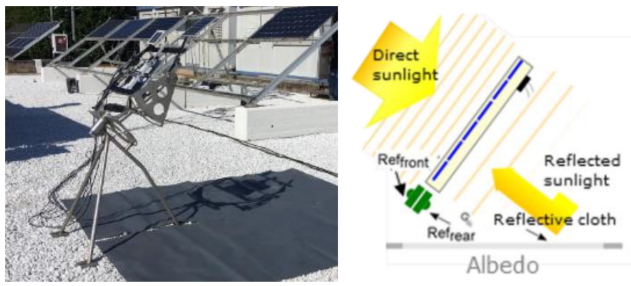

Fig. 4. Outdoor setup using different reflective grounds.

corrected". The diffuse reflector and double-source solar simulator approaches are illustrated in Fig. 2 and Fig. 3 respectively.

The third approach is based on double-sided outdoor measurements, extending a range of materials to adjust the ground albedo (Fig. 4). The TS suggests a matt reflective cloth to increase the surface uniformity, but it has been reported that this might increase the rear irradiance nonuniformity and other surfaces can be more appropriate [22]. The TS also sets limits on permissible deviations of operating conditions; in particular, the rear-side irradiance nonuniformity should be below 10% for outdoor measurements. In order to measure the nonuniformity of the rear-side irradiance for the outdoor measurements (also for indoor), at least the average of five symmetrically distributed points from a suggested matrix of nine points (e.g., *P*1-*P*3-*P*5-*P*7-*P*9, *P*2-*P*4-*P*5-*P*6-*P*8, etc.) needs to be selected as shown in Fig. 5 [7]. Similar to the indoor double-sided approach, in this method, besides the STC measurement at 1000 W/m^2 ($G_R = 0$ W/m^2), AM1.5 and 25 °C, $P_{\max}$ of the module shall be measured at 1000 W/m^2 $\pm$ 10% on the front side (or corrected to this value), plus different rear side irradiance levels G_{Ri} ($i = 1, 2, 3 \ldots$, for

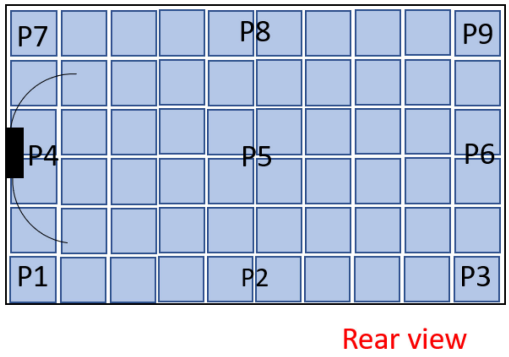

Fig. 5. Schematic representation of the positions for measuring the nonuniformity of the rear-side irradiance.

instance, $G_{\mathrm{R1}} < 100$ W/m^2, 100 W/m^2 $< G_{R2} <$ 200 W/m^2 and $G_{R3} >$ 200 W/m^2) and the BiFi coefficient is calculated as described previously [7].

III. Experimental Details

A. Device Characteristics

The device under test is a purpose constructed n-type glass-glass frameless four-cell (a cell area 16 cm $\times$ 16 cm) bifacial minimodule with a total area of 40 cm $\times$ 40 cm. The cells are connected in series and are arranged in a 2 $\times$ 2 matrix spaced similarly to a typical full-size module. The cells have a high bifaciality and were selected to ensure good current matching. There is no junction box and electrical connections are made directly to tabs exiting the side of the device. These features ensure that the device is intrinsically of high performance without mismatch effects in the *I–V* curves, which makes it ideal for this study of a range of measurement techniques for which irradiance nonuniformity is a challenging aspect.

B. Single-Side Illumination

I–V curve measurements were carried out at ESTI facilities using a class AAA PASAN IIIB PSS (pulse length of 10 ms) with the so-called multiflash (MF) method [23]–[25] in order to circumvent capacitive effects of the device [8] at 1000 W/m^2 and equivalent irradiance levels, (25.0 $\pm$ 0.1)°C and corrected to AM1.5. According to the standard IEC 60904-9 [26] the nonuniformity of the PSS used is 0.45% on a 3x3 m^2 area on the measurement plane for the incident light. A black opaque wooden panel was placed in direct contact with the rear surface of the device under test and to avoid residual or undesirable reflections of the incident light, the size of the test area was limited to that of the PV device under test using baffles (see Fig. 1). The setup, measurements procedure and rear-irradiance details have been reported previously [22]. The accredited measurement uncertainty for $P_{\max}$ measurements of bifacial devices on this simulator is 1.1%. The spectral responsivity of the module was measured using a differential spectral responsivity technique with a large area PSS equipped with several bandpass filters to obtain illumination of modules with quasi-monochromatic light

[27]. No significant differences between front and rear relative spectral responsivity were found.

C. Double-Sided Illumination: Single-Source + Rear Reflector

In order to ensure reproducibility of the measurements, the PV device was placed in a structure that allows placement of a high gloss white wooden reflective panel (optical reflectance $> 94\%$ in the wavelength 300 to 1200 nm) at various distances behind the module plane and parallel to it. By changing the distance and the area of the reflective panel, the rear irradiance was adjusted (see Fig. 2). For this particular case-study, the reflective rear panel with area A_2 has a size in the order of 15 times the minimodule effective area, A_1, and it was placed parallel and centred. For this single minimodule configuration, the light can be transmitted through the module by the spacing between the cells (see Fig. 2) and through the noncovered areas around the module and then scattered or reflected back from the back panel to the module contributing to the rear irradiance. In addition to the front side irradiance, the rear irradiance G_R was measured with a calibrated 2×2 cm^2 monocrystalline silicon reference cell with certified uncertainty UC ($k = 2$) of $\pm 0.48\%$. This reference cell was placed behind the module facing the reflective rear panel using a small holder to avoid minimize interference. The PSS (PASAN IIIB) used for the measurements exhibits a very good temporal stability with changes in the irradiance lower than 0.1% at 1000 W/m^2 from flash to flash. G_R and the *I–V* curves were measured separately but without changing the setup or measurement conditions. The front side irradiance was set to 1000 ± 1 W/m^2 without further corrections for the purpose of rear irradiance measurement only. Further details of the experimental setup are described in [21].

D. Double-Sided Illumination: Simultaneous Double Source Based on LED Bias Light

A simultaneous double-sided illumination solar simulator based on an existing large-area PSS combined with a low-cost prototype LED rear bias light was developed at ESTI [28]. The LED bias light can fulfil the standard requirements of rear illumination (0 to 400 W/m^2), nonuniformity ($\sim$4.45%) and temporal instability (both short term and long term instabilities are Class A, 0.45% and less than 0.25% (for 100 ms sweep time) over an illumination area of 60 cm $\times$ 60 cm according to the IEC 60904-9 [26]. A larger LED rear bias light for full size modules (100 cm $\times$ 170 cm) with a nonuniformity of class B is also being developed to better match the TS requirements [29]. The spectral irradiance of the LED bias light has been measured using a CAS140 spectroradiometer system in the range 300–1700 nm and is found to provide a poor match to the AM1.5 spectrum [29]. This would result in classification outside class C according to IEC 60904-9 [26]. A mismatch factor (MMF) of 1.1213 and 1.1353 for the front and rear-side of the module, respectively, was calculated. The poor spectral match can be compensated by a mismatch correction or by using the effective irradiance method defined in IEC 60904-7 [30]. For the double-sided measurements, the LED bias light structure is mounted vertically at the back of the device under test at an adjustable distance. The module to LED distance has been set at 50 cm for the tests reported here. This configuration enables illumination of the rear side by LED and front side by the PSS simultaneously. Separate single-side measurements are also possible. Identical data acquisition software and hardware system are used for both single- and double-side *I–V* measurements. In order to eliminate reflections between the two light sources, which might cause irradiance gain and nonuniformity, black masking and baffles around the module are used as recommended in the IEC TS 60904-1-2 [7].

E. Outdoor Measurements

The bifacial PV minimodule was placed in a specially designed rack with an elevation angle of 45°, and with the bottom of the module 1 m above ground level. The rack is sited at the ESTI facilities of the European Commission, in Ispra, northern Italy, at 220 m above sea level, considered to be a moderate subtropical climate (-10 °C to $+35$ °C, with less than 90% RH). The minimodule was measured close to noon under clear sky conditions with a front irradiance $G_{\text{front}} \sim 1000$ W/m^2 $\pm$ 10% and temperature and spectral corrections were performed. White reflective gravel (3 to 5 cm diameter stones) was taken to be the reference ground material with an albedo of 0.42 ± 0.04. The ground albedo was controlled and then modified using different selected materials (white stones, grey cloth, and black panels) in order to vary the rear irradiance to values above 50 W/m^2 [22] to obtain a suitable range of ground albedos and aiming for a nonuniformity of the rear irradiance below the value of 10% as specified in the TS [31]. The front and rear irradiance was monitored with calibrated sensors. The rear irradiance and nonuniformity of the rear irradiance for this specific site location has been studied and reported previously and it has been shown to depend on the ground material; the G_R nonuniformity may be also increased considerably beyond the permissible limit of 10% [22], [31]–[33]. The nonuniformity is defined as [26]

$$G_{\text{rear}}\ \text{Non} - \text{uniformity}\ (\%) = \frac{G_{\text{rear max}} - G_{\text{rear min}}}{G_{\text{rear max}} + G_{\text{rear min}}} \cdot 100 \tag{6}$$

where $G_{\text{rear max}}$ is the maximum irradiance in the rear-side and $G_{\text{rear min}}$ is the minimum irradiance in the rear-side.

One interesting exercise is to check the agreement between the double-sided illumination measurement and the addition (by using (2) with the $P_{\max}$ or I_{sc}) of the measurements of each side of the device obtained independently; i.e., the measurement of the front side with the rear side covered with a black panel and the rear side facing the ground with the front side covered with a black panel. In order for the sequential measurements to be comparable they were performed within a 2–3 min time interval, and a final double-sided measurement was also made to verify that conditions such as irradiance and module temperature had not changed to a significant extent. Prior to the test the device temperature was brought to close to 25 °C and the small experienced temperature fluctuations due to heating of the

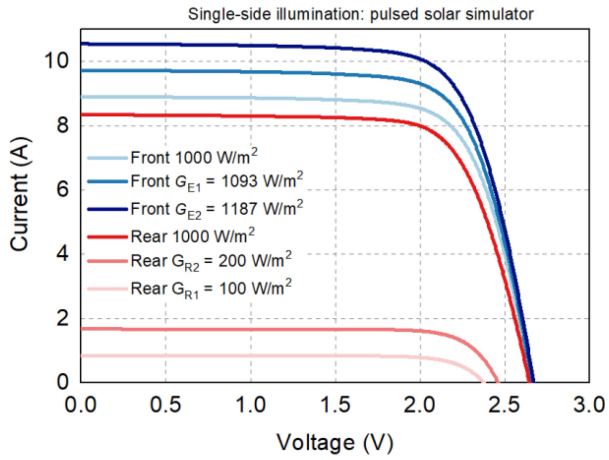

Fig. 6. Single-side illumination *I–V* curves measured with a PSS at different equivalent irradiance levels for both front and rear.

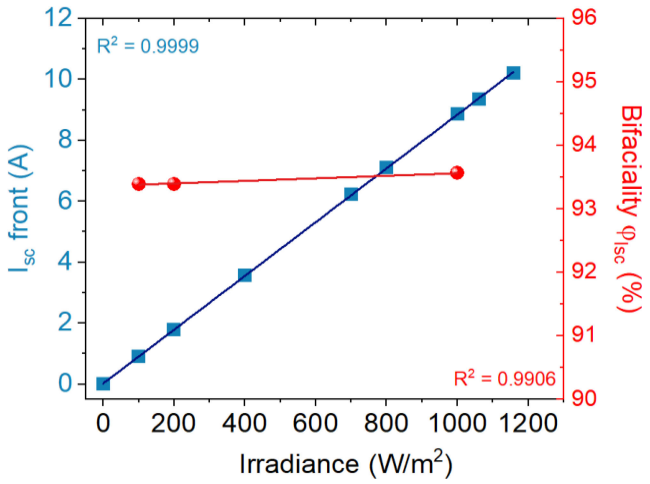

Fig. 7. I_{sc} and I_{sc} bifaciality coefficient as a function of front irradiances for single-side illumination approach.

order of 2 °C were corrected by using temperature coefficients previously measured indoors.

IV. Results and Discussion

A. Single-Side Illumination Measurements

I–V curves of the minimodule have been performed following the procedures, protocols and operating instructions accredited by Accredia (Italian National Accreditation body) for the calibration of bifacial PV devices at STC and equivalent irradiance levels G_{Ei} with a PSS. This accreditation guarantees accurate and reliable measurements for the single-side illumination approach for bifacial PV devices meeting the requirement of the ISO/IEC 17025:2017 and IEC TS 60904-1-2 standards and provides a reference for comparison. Fig. 6 shows the *I–V* curves measured for the minimodule illuminating the front and rear sides, respectively, and covering the nonilluminated surface at several equivalent and rear irradiances. As shown in Fig. 6, there are no deformations or kinks in the *I–V* curves of the minimodule that are often reported for full size modules due to cell mismatch or rear-side partial shading from junction boxes or frames (the minimodule has neither) [34].

From these values, an average I_{sc} bifaciality factor $\varphi_{Isc} = 93.45 \pm 0.95\%$ is obtained. The I_{sc} as a function of the front irradiance is plotted in Fig. 7. Linearity of the dependency of I_{sc} with irradiance for the entire range of values of interest (0 to 1200 W/m^2) with a $R^2 = 0.9999$, is observed, which is also observed for the I_{sc} of the rear side. It is noted that this analysis of linearity is purely mathematical and is not verified according to the latest version of IEC 60904-10 [35]. This result supports the use of I_{sc} values as a reliable proxy for irradiance in situations where its direct measurement may be difficult. Fig. 7 also shows the bifaciality coefficient for I_{sc}, φ_{Isc} (%), as a function of the front irradiance. A slight decrease of the bifaciality is noted for very low irradiances, but the difference is well within the measurement uncertainty.

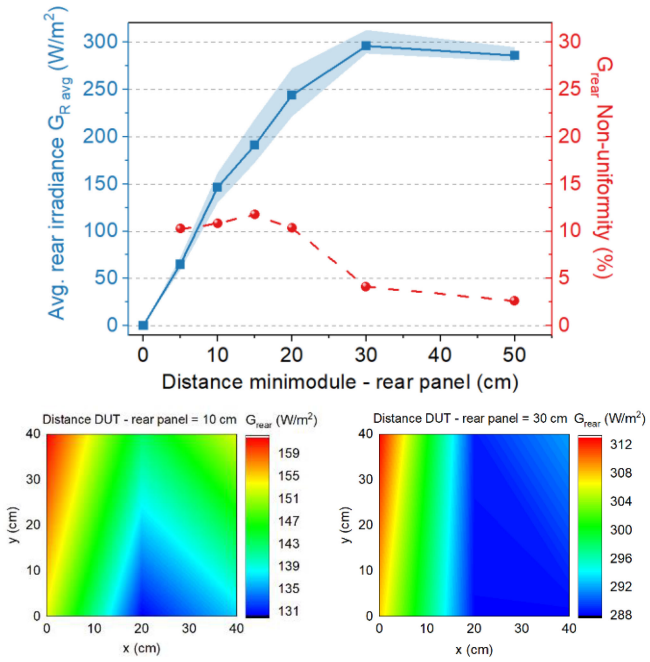

Fig. 8. Average rear irradiance $G_{r\ avg}$ (W/m^2) measured with a calibrated reference cell and the G_{rear} nonuniformity (%) for the double-sided illumination using a reflective rear panel. The Rear irradiance distribution maps for two distances between the device under test and the reflective panel are also shown.

B. Double-Sided Illumination: Single-Source+Rear Reflector Measurements

Fig. 8 shows the average rear irradiance $G_{R\ avg.}$ and the G_R nonuniformity as a function of the distance between the device under test and the reflective rear panel. The maximum and minimum G_R values measured over the module area are represented by the pale blue shaded areas. By changing the distance between the device under test and the reflective rear panel, the rear irradiance also changes and therefore can be adjusted to different values as desired to a maximum value of nearly 300 W/m^2. G_R increases with the distance between the

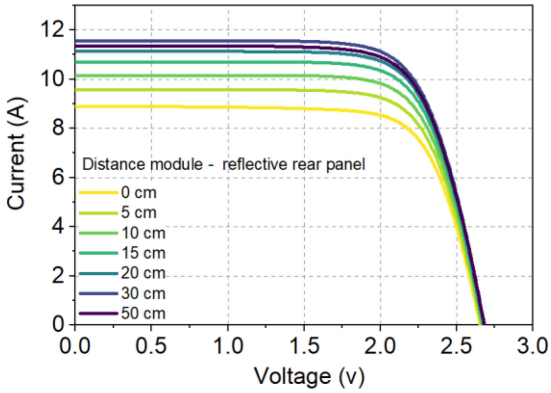

Fig. 9. *I–V* curves for the minimodule measured with the double-sided illumination approach using the reflective rear panel.

rear reflective panel and the module up to a maximum value (30 cm) and then slightly decreases. The explanation for this behavior depends on several factors influencing the intensity and spatial distribution of the light arriving at the panel and the angular and spatial distribution of the light reflected from the panel onto the rear side of the module. An analysis of these effects is outside the scope of the present article. Fig. 8 also shows that the G_{R} nonuniformity is slightly above 10% for DUT to reflective panel distances below 20 cm and then decreases to below 5% as the distance increases above 30 cm. The rear irradiance distribution maps for two specific distances between DUT and reflective panel are also plotted in Fig. 8. A spatial gradient of irradiance higher at the left side of the minimodule (view from the rear-side), which is most likely due to the relative geometry of the simulator light source, baffles, DUT, and the reflective rear panel. The use of reflective rear panels behind the minimodule increases the rear irradiance, and in doing so increases the $P_{\max}$ output power of the minimodule as shown in Fig. 9. The increase of the I_{sc} and $P_{\max}$ is observed with the distance between the DUT and the reflective panel. It is to be noted that the obtained level of irradiance nonuniformity on the rear side of the DUT does not cause noticeable deformations or kinks in the measured *I–V* curves.

This double-sided illumination approach with a single-source simulator and a reflective rear panel fulfils the IEC TS 60904-1-2 requirement for a solar simulator with adjustable irradiance levels for double-sided illumination. However, the TS also states that the nonuniformity of irradiance must be below 5% on both sides, at the irradiance levels used for the characterization of bifacial devices and those values used for corrections and uncertainty evaluation. As shown in Fig. 8, the G_R nonuniformity is higher than the allowed limit of nonuniformity for most of the distances between DUT and reflective panel. In order to reduce the G_R nonuniformity for low irradiances, improvements could be made in terms of different Lambertian reflective materials, panel sizes, etc.

In addition, the TS states for the indoor power generation gain with double-sided illumination: "Reflections between the two light sources may add irradiance nonuniformity. This may generate significant offsets between single-side and double-sided measurement methods results. In this case, double-sided illumination results must be corrected." However, there is not a clear definition on which approaches might be used for such correction. As shown previously, one of the main issues in double-sided illumination methods is the correct determination of the G_R to obtain an accurate BiFi coefficient value. As shown in Section III.A, the I_{sc} increases linearly with the irradiance, and a calculation of the G_R is possible by using the I_{sc} of the measured *I–V* curves

$$G_{E\ \mathrm{measured}}\left(\frac{w}{m^2}\right) = \frac{I_{\mathrm{sc\ @distances\ DUT-rear\ panel}}\ (A)}{I_{\mathrm{sc\ @STC}}\ (A)} \cdot 1000\left(\frac{W}{m^2}\right). \tag{7}$$

By using (2)

$$G_{Ei} = 1000 + \varphi \cdot G_{Ri}\ (w/\mathrm{m_2})\,.$$

The effective rear irradiance, $\mathrm{G_{R\ effective}}$, can be obtained

$$G_{R\ \mathrm{effective}\ \left(\frac{W}{\mathrm{m}^2}\right)} = \left[G_{E\ \mathrm{mesured}}\left(\frac{W}{\mathrm{m}^2}\right) - 1000\left(\frac{W}{\mathrm{m}^2}\right)\right] /\varphi \tag{8}$$

where $I_{\mathrm{sc\ @distances\ DUT\text{-}rear\ panel}}$ is the short circuit current obtained from the *I–V* curves measured with the double-sided illumination method by using a single-side source and the reflective rear panel at differences distances between the DUT and the reflective panel (and then different irradiances), $I_{\mathrm{sc\ @STC}}$ is the short circuit current at STC conditions for the front side (covering the rear side, that is, $G_R = 0$ W/m^2), G_{Ei} is the equivalent irradiance level, G_{Ri} is the rear irradiance, φ is the bifaciality coefficient and G_R effective is the rear irradiance calculated assuming linear dependency with I_{sc}. This correction increases the G_R with respect to the $G_{R\ \mathrm{avg}}$ to values close to the maximum G_R measure with the ref. cell and change the BiFi coefficient. A possible explanation for this change in G_R can be the fact that *I–V* curves are performed without the rear reference cell that might block/cover the light passing through the module/cell contributing to the rear irradiance and thus to the device performance. Since it is not possible to measure at the same time the rear irradiance and the device performance without shading the rear surface with the reference cell and thus affecting the performance measurement, this leads to a higher uncertainty in the determination of the G_R. The calculation of the BiFi coefficient will be shown in Section IV-E. However, Table I shows the $P_{\max}$ variation between single-side illumination at equivalent irradiance levels G_E and the calculated $P_{\max}$ from (4) and (5) by using the BiFi coefficients obtained with the measured average G_R and the effective G_R for a double-sided illumination with a reflective rear reflector. The variation in $P_{\max}$ increased with the rear irradiance but is strongly reduced to values between 0.4% to 0.7% when the effective G_R is used. These results show that the definition and measurement of the rear irradiance is crucial for the accurate determination of the parameters requested by the TS for double-sided illumination approaches and need to be reviewed to better account for intrinsic technical limitations.

TABLE I
P_{MAX}, DIFFERENCES BETWEEN SINGLE-SIDE ILLUMINATION AT EQUIVALENT IRRADIANCE LEVELS G_E AND THE CALCULATED P_{MAX} FROM (4) AND (5) USING THE BIFI COEFFICIENT FOR A DOUBLE-SIDED ILLUMINATION WITH A REFLECTIVE REAR REFLECTOR

φ (%)	G_R (W/m^2)	G_E (W/m^2)	P_{max} G_E (W)	*BiFi*	P_{max} $BiFi_{GR}$ (W)	ΔP_{max} (%)
			With $G_{R\,avg}$			
	0	1000	17.43		17.43	+0
93	100	1093	18.96	0.018	19.23	+1.42
	200	1187	20.50		21.03	+2.59
			With $G_{R\,effective}$			
	0	1000	17.43		17.43	+0
93	100	1093	18.96	0.016	19.03	+0.37
	200	1187	20.50		20.63	+0.63

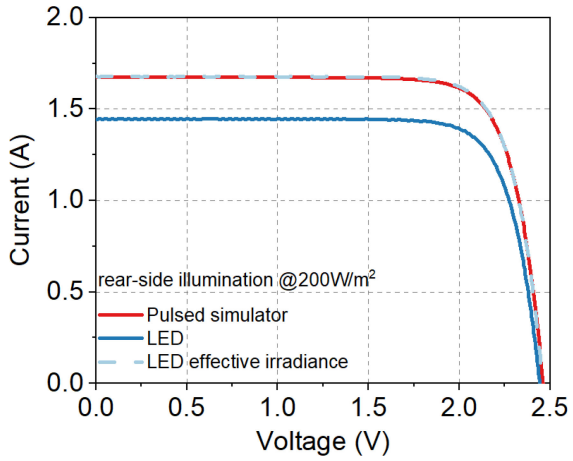

Fig. 10. *I–V* curves for the rear-side of the bifacial module using the PSS and LED bias light at 200 W/m^2 with and without effective irradiance adjustment.

C. Double-Sided Illumination: Simultaneous Double Source With LED Bias Light

I–V characteristics of the bifacial minimodule were measured using both the PSS with a multiflash method and LED bias light independently as well as in combination. The first step was to adjust and optimize the part corresponding to the LED bias light illumination and then the double-sided source system. Fig. 10 shows the *I–V* curves of the rear-side of the DUT at 200 W/m^2 with black cover by using the PSS and LED bias light separately. The *I–V* curve measured using the PSS at 200 W/m^2 is MMF corrected and is notably higher than the *I–V* curve measured at 200 W/m^2 using the LED bias light mainly due to the poor spectral content of the LEDs, which leads to a large MMF. In order to correct this spectral mismatch, the effective irradiance correction method, stated in Section IV of Standard IEC 60904-7 [30], may be applied [10]. The effective irradiance to generate the I_{sc} in the bifacial minimodule as generated at 200 W/m^2 is calculated as

$$G_{\text{eff}} = G_{\text{ref}} \cdot \text{MMF} \tag{9}$$

where G_{eff} (W/m^2) is the effective irradiance, G_{ref} (W/m^2) is the reference irradiance (in this particular case 200 W/m^2)

TABLE II
COMPARISON OF ELECTRICAL PARAMETERS MEASURED WITH THE EQUIVALENT IRRADIANCE SINGLE-SIDE METHOD BY A PSS AND DOUBLE-SIDE ILLUMINATION METHOD USING THE LED SIMULATOR

	I_{sc} (A)	V_{oc} (V)	P_{max} (W)	ΔI_{sc} (%)	ΔV_{oc} (%)	ΔP_{max} (%)
PSS 1187 W/m^2	10.51	2.67	20.50	-	-	-
PSS 1000 W/m^2 + LED 200 W/m^2	10.57	2.67	20.65	0.60	0.04	0.77
PSS 1000 W/m^2 + LED 200 W/m^2 corrected	10.53	2.67	20.55	0.20	0.05	0.29

and MMF is the mismatch factor of the device under LED illumination [see Section III-D]. However, because the MMF correction in this case is so large, and very sensitive to the accuracy of the measured LED spectrum, a different approach is employed. Since an accurate measurement at 200 W/m^2 of the rear-side of the DUT is available from the PSS, an analogous but improved approach is to use this measurement as a reference. By adjusting the voltage control, and hence intensity of the LEDs, an effective irradiance is applied such that the short circuit current is matched to that obtained using the PSS effectively correcting for the spectral mismatch and avoiding the necessity to correct the measurements mathematically. As can be seen from Fig. 10, the two *I–V* curves measured by the PSS and LED "effective irradiance" (red and light blue, respectively) are virtually indistinguishable.

The equivalent rear irradiance driven power gain yield measurement with single-side illumination described in IEC TS 60904-1-2 is used as the reference measurement to validate the LED-based bias light when used for double-sided illumination. The two measurement methods led to similar *I–V* characteristics for the minimodule, but the double-side illumination showed around 0.6% higher I_{sc} compared to single-side equivalent irradiance method as given in Table II.

Single-side measurements with and without black rear cover were made for the PSS and LED-based bias light. A gain of about 0.6% in I_{sc} is observed when the PSS is used without a rear cover [22] as compared to the case with the rear cover. This difference is most likely due to the portion of the light that passes through the module being reflected from the closely located LEDs and the LED mounting structure. On the other hand, there is no significant difference (less than 0.1%) between measurements with and without black rear cover when the LED-based bias light is used. This is because the portion of the light that passes through the module does not reflect to any significant extent from the distant PSS light source. The difference closely matches the extra I_{sc} of the double-side illumination compared to the single-side equivalent irradiance measurement, demonstrating that the gain is mainly due to stray/parasitic reflection from the back of the minimodule at the LED side. Table II gives electrical characteristics obtained using the two methods for

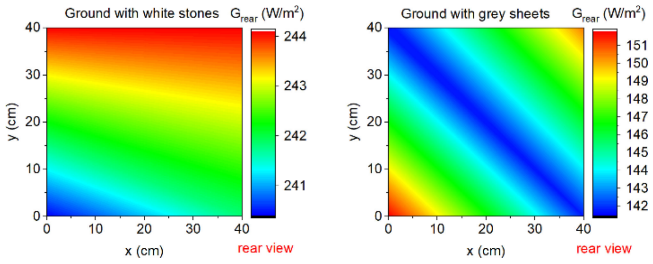

Fig. 11. Rear irradiance distribution maps for two outdoor ground materials, white gravel and grey sheets obtained at solar noon.

the bifacial minimodule. The main differences between two methods are in the $I_{\rm sc}$ and $P_{\rm max}$, 0.6% and 0.77%, respectively. A correction as proposed in IEC TS 60904-1-2 is performed on the double-side illumination measurements to compensate for the stray/parasitic reflected light. After correction the difference between the methods is less than 0.3% for $I_{\rm sc}$ and $P_{\rm max}$. The PV device used for testing purposes had a very good bifaciality coefficient and good rear-side cell current matching, so the *I–V* curves obtained with single-side illumination method were practically identical to those obtained with the double-sided method. For modules having poorer rear-side performance, the double-sided illumination approach may be necessary in order to obtain valid results, confirming the utility of the LED-based bias light approach.

D. Double-Sided Illumination Measurements in Outdoor Conditions

Fig. 11 shows the rear irradiance distribution maps for two representative examples of ground materials in the outdoor test facility, white stones, and grey sheets, respectively. In the first case, an average measured $G_R = 242$ W/m^2 (for a front irradiance of 952 W/m^2) and a nonuniformity of irradiance on the rear side of 0.8% was obtained at around solar noon. In the second example, an average $G_R = 146$ W/m^2 (for a front irradiance of 924 W/m^2) with a nonuniformity on the rear side of 3.5% was found. For all the ground material tested for outdoor conditions, the nonuniformity of the irradiance on the rear side was found to be below 5%**.** It should be noted that while such low levels of rear side nonuniformity are readily achievable for the minimodule, this is not the case for larger modules. While the impact of significant levels of rear side nonuniformity is outside the scope of the present article, it will have an impact on the performance of larger modules [36]–[39]. The measured values of the rear irradiance are used to plot the $P_{\rm max}$ as a function of G_R in order to calculate the BiFi coefficient. However, we can also define an effective rear irradiance obtained from the *I–V* curve parameters (as opposed to from a direct measurement) as

$$\text{Effective } G_R = \frac{I_{\text{sc\_rear only,outdoor}}}{I_{\text{sc\_rear indoor STC}}} \cdot 1000 \text{ W/m}^2 \quad (10)$$

where $I_{\text{sc rear only}}$, outdoor is the short-circuit current measured covering the front side with a black panel in outdoor conditions and $I_{\text{sc rear indoor STC}}$ is the rear side short-circuit current measured at STC under indoor conditions covering the

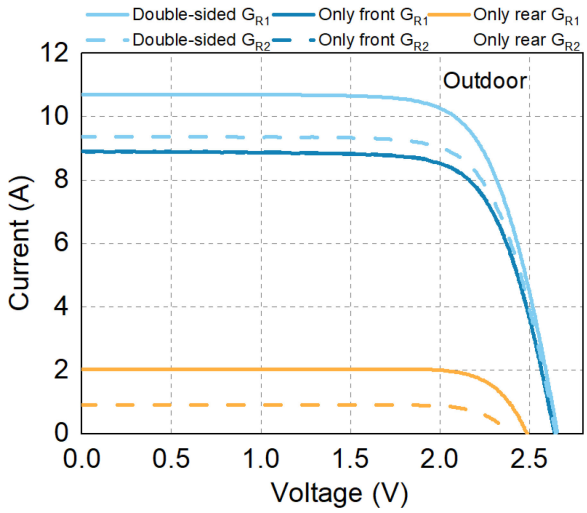

Fig. 12. *I–V* curves of the double-sided illumination, only the front side (rear side covered) and only rear side facing the ground (front side covered) for two examples of rear irradiance G_R.

nonilluminated side (front as defined by manufacturer) with a black panel. In this case-study of a minimodule, the difference between the measured and the calculated equivalent irradiance level G_E, is relatively low, ranging from 1.1% to 1.7%. As will be shown in the following section, this implies a slight variation of the BiFi coefficient value. The accurate and reliable calculation of the G_R in outdoor conditions is the main issue to be considered in this approach for the characterization of bifacial PV devices as reported in [22] and [36].

The operating conditions in the outdoor approach are less controllable than for indoor methods due to the parasitic reflection of the environment. The *I–V* curves of the double-sided, front side only and rear side only measurements for two representative G_R obtained at solar noon are plotted in Fig. 12. The absence of any mismatch or kink on the *I–V* curves is noted and this is due to the minimal partial ground shading of the small device and mounting structure which leads to a low nonuniformity of the irradiance on the rear side. The electrical parameter of the $P_{\rm max}$ and $I_{\rm sc}$ for the front side, rear side and double-sided together with the calculated $P_{\rm max}$ or $I_{\rm sc}$ by adding front only and rear only $P_{\rm max}$ (or $I_{\rm sc}$) are given in Table III. The variation between the measured double-sided and the calculated $P_{\rm max}$ (or $I_{\rm sc}$) seems to be uncorrelated to the rear irradiance suggesting that there is no systematic error due to corrections. $\Delta P_{\rm max}$ varied from -0.38% to $+1.03\%$, differences that can be considered to be of the same order of magnitude as the measurement uncertainty for outdoor measurements. The double-sided measurement is greater than the addition of the two contributions, front and rear, likely due to the light passing through the module contributing to the total incident light (that it is blocked when a black panel is used). However, the black panel used for covering the front (or rear surface for the single-side measurement in outdoor) might also contribute to the irradiance if there is a gap ($>$1 cm) between the module and the panel. In any case, the difference is small enough to be considered to be within the measurement uncertainty.

TABLE III
P_{MAX} AND I_{SC} OBTAINED FROM DOUBLE-SIDED ILLUMINATION, ONLY FRONT SIDE AND ONLY REAR SIDE (WITH THE OTHER SIDE COVERED, RESPECTIVELY) AND THE CALCULATED P_{MAX} FROM THE PREVIOUS VALUES

P_{max} front (W)	P_{max} rear (W)	P_{max} double (W)	$P_{max} = P_{max\ front} + P_{max\ rear}$ (W)	ΔP_{max} (%)
16.93	4.08	20.85	21.01	0.77
16.90	3.73	20.64	20.63	-0.05
16.90	2.70	19.40	19.6	1.03
16.58	1.76	18.41	18.34	-0.38

$I_{sc\ front}$ (W)	$I_{sc\ rear}$ (W)	$I_{sc\ double}$ (W)	$I_{sc} = I_{sc\ front} + I_{sc\ rear}$ (W)	ΔI_{sc} (%)
8.67	2.02	10.69	10.69	0.00
8.63	1.87	10.59	10.5	-0.85
8.62	1.35	9.93	9.97	0.40
8.46	0.90	9.37	9.36	-0.11

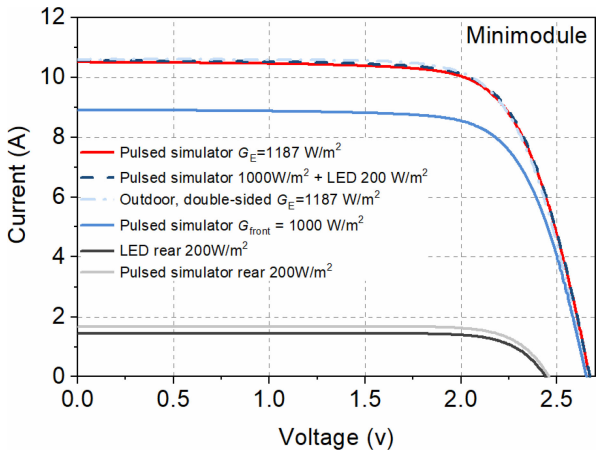

Fig. 13. *I–V* curves measured with the single-side illumination, double-source with LED and the outdoor methods.

E. Comparison of Characterisation Approaches

I–V curves measured approximately at equivalent irradiance level $G_E = 1187$ W/m^2 with three different approaches, single-side illumination, outdoor double-sided and double-source illumination with a LED rear bias light are plotted in Fig. 13. *I–V* curves for STC front and 200 W/m^2 illuminating the rear side are also plotted for single-sided and the LED bias light. A good agreement between the curves at this particular G_E is observed. In order to compare in detail the different approaches, Table IV gives the P_{max} variation with respect to the single-side illumination approach (used as reference method). A good agreement among the different characterisation methods with a variation below 0.8% (within the 1.1% P_{max} measurement uncertainty of the single-sided method) is observed. An outlier is obtained for a double-sided illumination approach with a rear reflector when the measured average rear irradiance is used. In this case, P_{max} is overestimated by +2.6%. As mentioned, this is expected to be due to the higher G_R nonuniformity and the uncertainty in the G_R measurement in this method and might be improved by changing the specular reflective rear panel by a larger Lambertian reflector material. In any case, this approach

TABLE IV
P_{MAX}, VARIATION WITH RESPECT TO THE SINGLE-SIDE EQUIVALENT IRRADIANCE LEVEL METHOD AT $G_{Ei} = 1187$ W/M^2 FOR THE DIFFERENT CHARACTERIZATION APPROACHES

G_{Ei} =1187 W/m²	P_{max} (W)	ΔP_{max} (%)
Pulsed simulator	20.50	+0.00
Pulsed simulator + LED	20.55	+0.25
Rear reflector $G_{R\ avg}$	21.03	+2.59
Rear reflector $G_{R\ effective}$	20.67	+0.83
Outdoor	20.64	+0.68

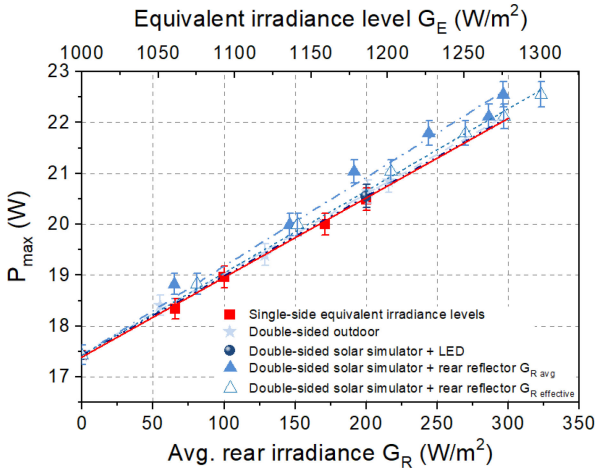

Fig. 14. P_{max} as a function of the average irradiance level on the rear G_R (bottom *x*-axis) or its single-sided equivalent irradiance G_E (top *x*-axis).

TABLE V
REAR IRRADIANCE DRIVEN POWER GAIN YIELD, BIFI, FOR THE DIFFERENT APPROACHES

Method	*BiFi* (W/Wm^{-2})
Pulsed simulator	0.0152 ± 0.0014
Pulsed simulator + LED	0.0156 ± 0.0014
Rear reflector $G_{R\ avg}$	0.0178 ± 0.0014
Rear reflector $G_{R\ effective}$	0.0163 ± 0.0014
Outdoor	0.0160 ± 0.0014

showed the largest deviation from the reference method and it can be considered the least reliable approach due to the difficulties to control the reflected irradiance [15].

Fig. 14 shows the P_{max} as a function of the average rear irradiance G_R or its single-side equivalent irradiance G_E, and the BiFi coefficient calculated from the slope of the curve. The four different approaches analyzed in this article have been plotted including the correction of the double-sided illumination approach with a rear reflector using the effective G_R. This is a good method to compare the different approaches assuming the single-side illumination approach as the reference one. In general, an excellent agreement in BiFi coefficient is observed for the different methods mainly due to the low uncertainty in the rear irradiance measurement (due to its relatively small size). Values ranged from 0.0152 to 0.0178 W/Wm^{-2} with an uncertainty of 0.0014 W/Wm^{-2} as given in Table V. As mentioned previously, the double-sided illumination approach

with a reflective rear panel using the average G_R showed a larger deviation with a BiFi value of 0.0178. In addition, the upscaling of this method leads to larger nonuniformity in G_R as reported for full size modules [21]. Note that the BiFi coefficient is strongly dependent on the rear irradiance measurement for outdoor and double-sided illumination showing important differences if the average, minimum or effective irradiance are used and care needs to be taken on the G_R measurement [22], [36].

V. Conclusion

A bifacial c-Si PV minimodule was measured with different characterization approaches at the ESTI facilities according to the recently published IEC TS 60904-1-2. For the bifacial device under test, all the characterization methods proposed in the TS were feasible. Deviations below 0.83% with respect to the reference testing method (below the measurement uncertainty of the solar simulator for single-side illumination method) were obtained except for the double-source method with rear reflector and $G_{R\ \mathrm{avg}}$ which has larger deviations. The different approaches resulted in a good output power agreement especially considering the limitations inherent in obtaining low rear side irradiance nonuniformities and the difficulties in measuring the rear irradiance for double-sided illumination approaches. The variations in the results with respect to the considered reference method (single-side illumination with equivalent irradiance levels) may help in future uncertainty analysis depending on the particular approach. Double-sided illumination with a reflective rear panel raised concerns about the possible difficulties in the quantification of the effects on the rear irradiance caused by light source geometry and light transmittance and their standardization. Double-sided illumination using LED bias light led to an excellent agreement with the reference method. However, the difficulty of obtaining a good spectral match and avoiding the use of corrections (effective irradiance) using the most readily available LEDs raises concerns about the feasibility of this approach to obtain absolute $P_{\max}$ values, although it would already be suitable for BiFi measurements. The obtained results will provide useful feedback to the IEC Technical Committee 82 Working Group 2 for future improvements of the TS. Such improvements should focus on the influence of the rear irradiance nonuniformity, and suitability and feasibility of the different approaches for full size modules. The rear side nonuniformity is generally found to be much higher in real outdoor conditions than that experienced for the minimodule. The effect of significant nonuniformity is outside the scope of the present article, which is intended to compare the different measurement approaches in as close to optimum conditions as possible. For this reason, the validity of the 10% rear side nonuniformity limit for outdoor measurements specified in the TS has not been scrutinized. Nevertheless, the results of the double-sided illumination approach with a reflective rear panel, as well as other reported work on outdoor mounted modules, demonstrate that as nonuniformity increases so does its impact on performance. The practicality of testing larger modules in accordance with the TS in outdoor conditions will therefore be a challenge. Finally, the TS recommends different acceptable levels of rear side nonuniformity for the double-sided illumination approaches depending on whether they are indoor or outdoor. Different nonuniformity levels in different tests will make comparison more difficult and alignment of this requirement for the different double-sided illumination approaches would be desirable to enable all approaches to be fully comparable.

Acknowledgment

The authors would like to thank Mr. F. Noseda for the technical support and Dr. B. V. Aken from ECN part of TNO (The Netherlands) for providing the minimodule.

References

[1] J. Stein *et al.*, "Bifacial photovoltaic modules and systems: Experience and results from international research and pilot applications," *IEA PVPS Task 13 Perform., Oper. Rel. Photovolt. Syst.*, 2021.
[2] H. Apostoleris, A. Al Ghaferi, and M. Chiesa, "What is going on with middle eastern solar prices, and what does it mean for the rest of us?," *Prog. Photovolt. Res. Appl.*, 2021, doi: 10.1002/pip.3414.
[3] C. D. Rodríguez-Gallegos *et al.*, "Global techno-economic performance of bifacial and tracking photovoltaic systems," *Joule*, vol. 4, no. 7, pp. 1514–1541, 2020.
[4] R. Kopecek and J. Libal, "Bifacial photovoltaics 2021: Status, opportunities and challenges," *Energies*, vol. 14, no. 8, 2021, Art. no. 2076.
[5] ITRPV-2021, *International Technology Roadmap for Photovoltaic (ITRPV)*, 2021.
[6] *Solar Photovoltaic Energy Systems – Terms, Definitions, and Symbols*, IEC TS 61836, 2016.
[7] *Measurement of Current-Voltage Characteristics of Bifacial Photovoltaic (PV) Devices*, IEC TS 60904-1-2, 2019.
[8] J. Lopez-Garcia and T. Sample, "Comparison of electrical performance of bifacial silicon PV modules," in *Proc. 33rd Eur. Photovolt. Sol. Energy Conf. Exhib.*, Sep. 2017, pp. 1432–1437.
[9] S. Roest, W. Nawara, B. B. Van Aken, and E. Garcia-Goma, "Single side versus double side illumination method IV measurements for several types of bifacial PV modules," in *Proc. 33rd Eur. Photovolt. Sol. Energy Conf. Exhib.*, 2017, pp. 1427–1431.
[10] C. Deline *et al.*, "Assessment of bifacial photovoltaic module power rating methodologies—Inside and out," *IEEE J. Photovolt.*, vol. 7, no. 2, pp. 575–580, Mar. 2017, doi: 10.1109/jphotov.2017.2650565.
[11] L. Pyrot *et al.*, "Bifacial module measurements with G_E method," in *Proc. 4th Bifacial Workshop BIFIPV*, Oct. 2017.
[12] H. Ossenbrink, H. Müllejans, R. Kenny, and E. Dunlop, "Standards in photovoltaic technology," in *Earth and Planetary Sciences*, Amsterdam, The Netherlands: Elsevier, 2012, pp. 787–803.
[13] C. Comparotto *et al.*, "Bifacial n-Type solar modules: Indoor and outdoor evaluation," in *Proc. 29th Eur. Photovolt. Sol. Energy Conf. Exhib.*, 2014, pp. 3248–3250.
[14] J. P. Singh, A. G. Aberle, and T. M. Walsh, "Electrical characterization method for bifacial photovoltaic modules," *Sol. Energy Mater. Sol. Cells*, vol. 127, pp. 136–142, 2014. [Online]. Available: http://dx.doi.org/10.1016/j.solmat.2014.04.017
[15] T. S. Liang *et al.*, "A review of crystalline silicon bifacial photovoltaic performance characterisation and simulation," *Energy Environ. Sci.*, vol. 12, no. 1, pp. 116–148, 2019.
[16] B. Newman *et al.*, "Comparison of bifacial module laboratory testing methods," in *Proc. 33rd Eur. Photovolt. Sol. Energy Conf. Exhib.*, 2017, pp. 1632–1635.
[17] Y. Zhang, Q. Gao, Y. Yu, and Z. Liu, "Comparison of double-side and equivalent single-side illumination methods for measuring the *I-V* characteristics of bifacial photovoltaic devices," *IEEE J. Photovolt.*, vol. 8, no. 2, pp. 397–403, Feb. 2018, doi: 10.1109/jphotov.2017.2778226.
[18] G. Razongles *et al.*, "Bifacial photovoltaic modules: Measurement challenges," in *Proc. 6th Int. Conf. Crystalline Silicon Photovolt.*, 2016, pp. 188–198.

[19] A. Schmid, G. Dulger, G. Baraah, and U. Kräling, "IV measurement of bifacial modules: Bifacial vs. monofacial illumination," in *Proc. 33rd Eur. Photovolt. Sol. Energy Conf. Exhib.*, Sep. 2017, pp. 1624–1627.

[20] B. Soria, E. Gerritsen, P. Lefillastre, and J. E. Broquin, "A study of the annual performance of bifacial photovoltaic modules in the case of vertical facade integration," *Energy Sci. Eng.*, vol. 4, no. 1, pp. 52–68, 2016, doi: 10.1002/ese3.103.

[21] J. Lopez-Garcia, A. Casado, and T. Sample, "Electrical performance of bifacial silicon PV modules under different indoor mounting configurations affecting the rear reflected irradiance," *Sol. Energy*, vol. 177, pp. 471–482, 2019.

[22] J. Lopez-Garcia, R. S. R. Gali, E. Grau-Luque, and T. Sample, "Assessment of the rear irradiance on bifacial silicon PV modules," in *Proc. 36th Eur. Photovolt. Sol. Energy Conf. Exhib.*, Sep. 2019, pp. 901–908.

[23] N. Ferretti, Y. Pelet, J. Berghold, V. Fakhfouri, and P. Grunow, "Performance testing of high-efficient PV modules using single 10 ms flash pulses," in *Proc. 28th Eur. Photovolt. Sol. Energy Conf. Exhib.*, Sep./Oct. 2013, pp. 3184–3187.

[24] J. Lopez-Garcia, B. Haile, D. Pavanello, A. Pozza, and T. Sample, "Characterisation of n-Type bifacial silicon PV modules," in *Proc. 32nd Eur. Photovolt. Sol. Energy Conf. Exhib.*, Jun. 2016, pp. 1724–1729.

[25] A. Virtuani *et al.*, "A fast and accurate method for the performance testing of high-efficiency C-Si photovoltaic modules using a 10 Ms single-pulse solar simulator," in *Proc. 38th IEEE Photovolt. Specialists Conf.*, 2012, pp. 496–500.

[26] *Photovoltaic Devices – Part 9: Classification of Solar Simulator Characteristics*, IEC 60904-9, 2007.

[27] R. Van Steenwinkel, "Measurements of spectral responsivities of cells and modules," in *Proc. 7th Eur. Photovolt. Sol. Energy Conf. Exhib.*, 1986, pp. 325–329.

[28] D. Shaw, J. Lopez-Garcia, R. Kenny, L. Pinero-Prieto, and E. Ozkalay, "Design study of a double-side illumination solar simulator for bifacial silicon PV modules characterisation based on low-cost LED bias light," in *Proc. 35th Eur. Photovolt. Sol. Energy Conf. Exhib.*, Sep. 2018, pp. 1001–1005.

[29] T. Lyubenova, R. P. Kenny, D. Shaw, D. Pavanello, and J. Lopez-Garcia, "Double-sided characterisation of full-size bifacial PV modules based on low-cost LED bias light," in *Proc. 38th Eur. Photovolt. Sol. Energy Conf. Exhib.*, Sep. 2021, Art. no. 4AV.2.23.

[30] *Computation of the Spectral Mismatch Correction for Measurements of Photovoltaic Devices*, IEC 60904-7, 2008.

[31] E. Ozkalay, J. Lopez-Garcia, L. Pinero-Prieto, A. Gracia-Amillo, and R. P. Kenny, "Evaluation of the non-uniformity of rear-side irradiance in outdoor mounted bifacial silicon PV modules," *Proc. AIP Conf. Proc.*, vol. 2147, 2019, Art. no. 020011.

[32] R. P. Kenny, J. Lopez-Garcia, E. G. Menendez, B. Haile, and D. Shaw, "Characterizing bifacial modules in variable operating conditions," in *Proc. 7th IEEE World Conf. Photovolt. Energy Convers.*, Jan. 2018, pp. 1210–1214.

[33] R. P. Kenny, E. G. Menendez, J. Lopez-Garcia, and B. Haile, "Characterizing the operating conditions of bifacial modules," in *Proc. 8th Int. Conf. Crystalline Silicon Photovolt.*, 2018.

[34] J. Lopez-Garcia, D. Pavanello, and T. Sample, "Analysis of temperature coefficients of bifacial crystalline silicon PV modules," *IEEE J. Photovolt.*, vol. 8, no. 4, pp. 960–968, Apr. 2018.

[35] *Photovoltaic Devices–Part 10: Methods of Linear Dependence and Linearity Measurements*, IEC 60904-10, 2020.

[36] E. Ozkalay, J. Lopez-Garcia, L. Pinero-Prieto, and R. P. Kenny, "Effect of outdoor rear-side irradiance non-uniformity on the performance of bifacial silicon PV modules," in *Proc. 9th Int. Conf. Crystalline Silicon Photovolt.*, Apr. 2019, pp. S3–04.

[37] G. Raina, R. Vijay, and S. Sinha, "Assessing the suitability of IV curve translation at varying irradiance and temperature range," *Sustain. Energy Technol. Assessments*, vol. 51, 2022, Art. no. 101925.

[38] Y. Tao *et al.*, "Parameterizing mismatch loss in bifacial photovoltaic modules with global deployment: A comprehensive study," *Appl. Energy*, vol. 303, 2021, Art. no. 117636.

[39] C. Deline, S. A. Pelaez, S. MacAlpine, and C. Olalla, "Estimating and parameterizing mismatch power loss in bifacial photovoltaic systems," *Prog. Photovolt. Res. Appl.*, vol. 28, no. 7, pp. 691–703, 2020.